



**MOTOROLA**

**MC4344  
MC4044**

**PHASE-FREQUENCY DETECTOR**

The MC4344/4044 consists of two digital phase detectors, a charge pump, and an amplifier. In combination with a voltage controlled multivibrator (such as the MC4324/4024 or MC1648), it is useful in a broad range of phase-locked loop applications. The circuit accepts TTL waveforms at the R and V inputs and generates an error voltage that is proportional to the frequency and/or phase difference of the input signals. Phase detector #1 is intended for use in systems requiring zero frequency and phase difference at lock. Phase detector #2 is used if quadrature lock is desired. Phase detector #2 can also be used to indicate that the main loop, utilizing phase detector #1, is out of lock.

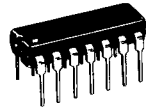
Operating Frequency = 8 MHz typ  
Input Loading Factor: R, V = 3  
Output Loading Factor (Pin 8) = 10  
Total Power Dissipation = 85 mW typ/pkg  
Propagation Delay Time = 9.0 ns typ  
(thru phase detector)

**PHASE-FREQUENCY  
DETECTOR**

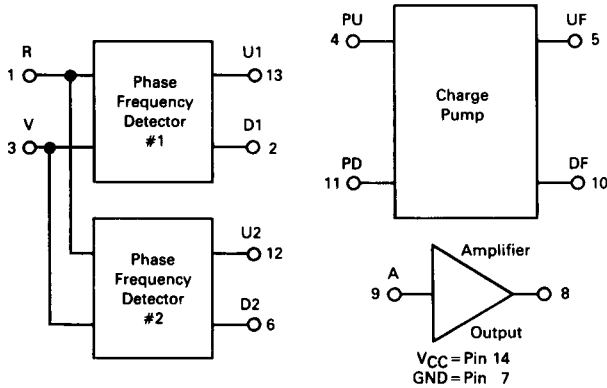


**L SUFFIX  
CERAMIC PACKAGE  
CASE 632  
(TO-116)**

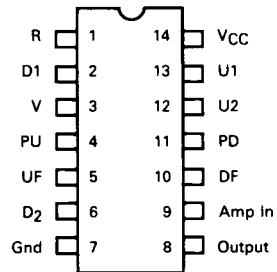
**P SUFFIX  
PLASTIC PACKAGE  
CASE 646  
MC4044 only**



**LOGIC DIAGRAM**

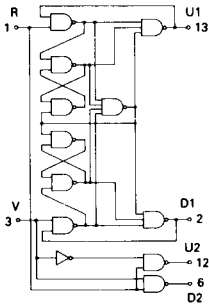


**PIN ASSIGNMENT**

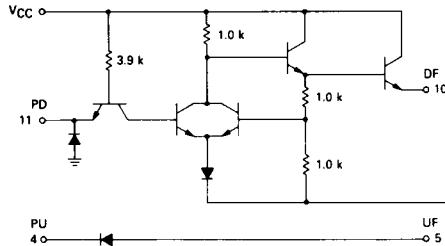


6

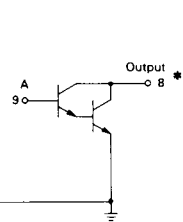
**PHASE DETECTOR**



**CHARGE PUMP**



**AMPLIFIER**



\*VMAX not to exceed 8.0 Vdc.





instance, outputs U1 and D1 remain unchanged. The input states next become R-V = 0-1; moving horizontally to the R-V = 0-1 column, stable state (2) is indicated. At this point there is still no change in U1 or D1. The next input change shifts operation to the R-V = 0-0 column where unstable state 5 is indicated. Moving vertically to stable state (5), the outputs now change state to U1-D1 = 1-1. The next input change, R-V = 1-0, drives the circuitry to stable state (8), with no change in U1 or D1. The next input, R-V = 1-1, leads to stable state (7) with no change in the outputs. The next two input state changes cause U1 to go low between the negative transitions of R and V. As the inputs continue to change, the circuitry moves repeatedly through stable states (2), (5), (8), (7), (2), etc., as shown, and a periodic waveform is obtained on the U1 terminal while D1 remains high.

A similar result is obtained if V is leading with respect to R, except that the periodic waveform now appears on D1 as shown in rows e-h of the timing diagram of Figure 2. In each case, the average value of the resulting waveform is proportional to the phase difference between the two inputs. In a closed loop application, the error signal for controlling the VCO is derived by translating and filtering these waveforms.

The results obtained when R and V are separated by a fixed frequency difference are indicated in rows i-l of the timing system. For this case, the U1 output goes low when R goes low and stays in that state until a negative transition on V occurs. The resulting waveform is similar

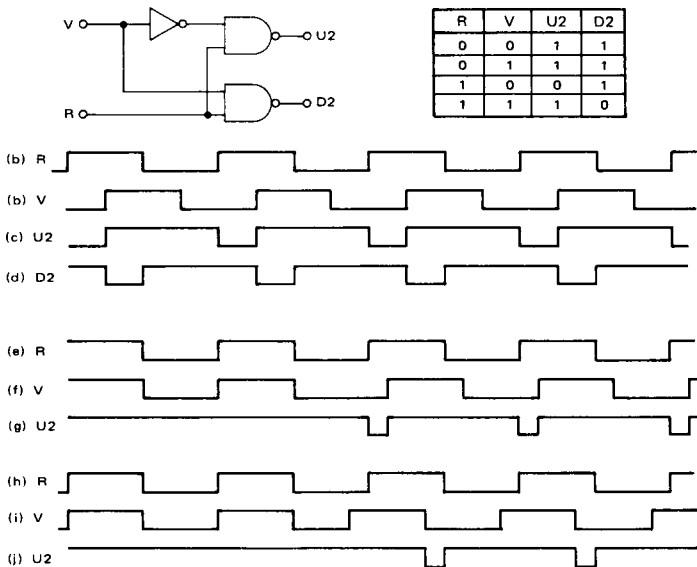
to the fixed phase difference case, but now the duty cycle of the U1 waveform varies at a rate proportional to the difference frequency of the two inputs, R and V. It is this characteristic that permits the MC4344/4044 to be used as a frequency discriminator; if the signal on R has been frequency modulated and if the loop bandwidth is selected to pass the deviation frequency but reject R and V, the resulting error voltage applied to the VCO will be the recovered modulation signal.

Phase detector #2 consists only of combinatorial logic, therefore its characteristics can be determined from the simple truth table of Figure 3. Since circuit operation requires that both inputs to the charge pump either be high or have the same duty cycle when lock occurs, using this phase detector leads to a quadrature relationship between R and V. This is illustrated in rows a-d of the timing diagram of Figure 3. Note that any deviation from a fifty percent duty cycle on the inputs would appear as phase error.

Waveforms showing the operation of phase detector #2 when phase detector #1 is being used in a closed loop are indicated in rows e-j. When the main loop is locked, U2 remains high. If the loop drifts out of lock in either direction a negative pulse whose width is proportional to the amount of drift appears on U2. This can be used to generate a simple loss-of-lock indicator.

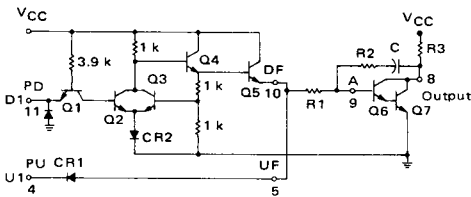
Operation of the charge pump is best explained by considering it in conjunction with the Darlington amplifier included in the package (see Figure 4). There will be

FIGURE 3 — PHASE DETECTOR #2 OPERATION



a pulsed waveform on either PD or PU, depending on the phase-frequency relationship of R and V. The charge pump serves to invert one of the input waveforms (D1) and translates the voltage levels before they are applied to the loop filter. When PD is low and PU is high, Q1 will be conducting in the normal direction and Q2 will be off. Current will be flowing through Q3 and CR2; the base of Q3 will be two  $V_{BE}$  drops above ground or approximately 1.5 volts. Since both of the resistors connected to the base of Q3 are equal, the emitter of Q4 (base of Q5) will be approximately 3.0 volts. For this condition, the emitter of Q5 (DF) will be on  $V_{BE}$  below this voltage, or about 2.25 volts. The PU input to the charge pump is high (> 2.4 volts) and CR1 will be reverse biased. Therefore Q5 will be supplying current to Q6. This will tend to lower the voltage at the collector of Q7, resulting in an error signal that lowers the VCO frequency as required by a "pump down" signal.

FIGURE 4 — CHARGE PUMP OPERATION



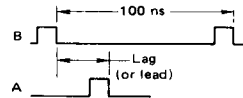
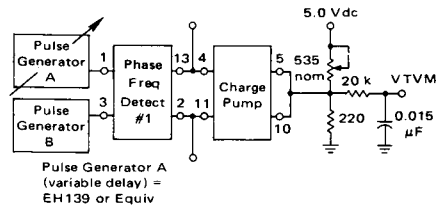
When PU is low and PD is high, CR1 is forward biased and UF will be approximately one  $V_{BE}$  above ground (neglecting the  $V_{CE(sat)}$  of the driving gate). With PD high, Q1 conducts in the reverse direction, supplying base current for Q2. While Q2 is conducting, Q4 is prevented from supplying base drive to Q5; with Q5 cut off and UF low there is no base current for Q6 and the voltage at the collector of Q7 moves up, resulting in an increase in the VCO operating frequency as required by a "pump up" signal.

If both inputs to the charge pump are high (zero phase difference), both CR1 and the base-emitter junction of Q5 are reverse biased and there is no tendency for the error voltage to change. The output of the charge pump varies between one  $V_{BE}$  and three  $V_{BE}$  as the phase difference of R and V varies from minus  $2\pi$  to plus  $2\pi$ . If this signal is filtered to remove the high-frequency components, the phase detector transfer function,  $K_{\phi}$ , of approximately 0.12 volt/radian is obtained (see Figure 5).

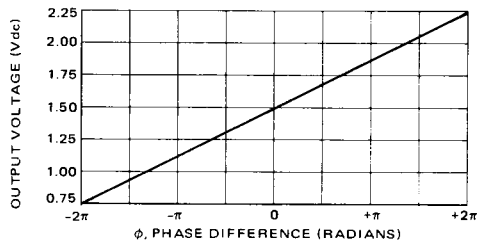
The specified gain constant of 0.12 volt/radian may not be obtained if the amplifier/filter combination is improperly designed. As indicated previously, the charge pump delivers pump commands of about 2.25 volts on the positive swings and 0.75 volt on the negative swings for a mean no-pump value of 1.5 volts. If the filter amplifier is biased to threshold "on" at 1.5 volts, then the pump up

and down voltages have equal effects. The pump signals are established by  $V_{BE}$ s of transistors with milliamperes of current flowing. On the other hand, the transistors included for use as a filter amplifier will have very small currents flowing and will have correspondingly lower  $V_{BE}$ s — on the order of 0.6 volt each for a threshold of 1.2 volts. Any displacement of the threshold from 1.5 volts causes an increase in gain in one direction and a reduction in the other. The transistor configuration provided is hence not optimum but does allow for the use of an additional transistor to improve filter response. This addition also results in a non-symmetrical response since the threshold is now approximately 1.8 volts. The effective positive swing is limited to 0.45 volt while the negative swing below threshold can be greater than 1.0 volt. This means that the loop gain when changing from a high frequency to a lower frequency is less than when changing in the opposite direction. For type two loops this tends to increase overshoot when going from low to high and increases damping in the other direction. These problems and the selection of external filter components are intimately related to system requirements and are discussed in detail in the filter design section.

FIGURE 5 — PHASE DETECTOR TEST



Shown for positive phase angle. Reverse A and B for negative phase angle.



**PHASE-LOCKED LOOP COMPONENTS**

**General**

A basic phase-locked loop, when operating properly, will acquire ("lock on") an input signal, track it in frequency, and exhibit a fixed phase relationship relative to the input. In this basic loop, the output frequency will be identical to the input frequency (Figure 6). A fundamental loop consists of a phase detector, amplifier/filter, and voltage-controlled oscillator (Figure 7). It appears and acts like a unity gain feedback loop. The controlled variable is phase; any error between  $f_{in}$  and  $f_{out}$  is amplified and applied to the VCO in a corrective direction.

**FIGURE 6 — BASIC PHASE-LOCKED LOOP FREQUENCY RELATIONSHIP**

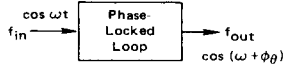
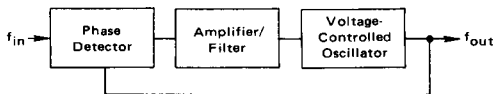


**FIGURE 7 — FUNDAMENTAL PHASE-LOCKED LOOP**



Simple phase detectors in digital phase-locked loops usually put out a series of pulses. The average value of these pulses is the "gain constant,"  $K_φ$ , of the phase detector — the volts out for a given phase difference, expressed as volts/radian.

The VCO is designed so that its output frequency range is equal to or greater than the required output frequency range of the system. The ratio of change in output frequency to input control voltage is called "gain constant,"  $K_V$ . If the slope of  $f_{out}$  to  $V_{in}$  is not linear (i.e., changes greater than 25%) over the expected frequency range, the curve should be piece-wise approximated and the appropriate constant applied for "best" and "worst" case analysis of loop performance.

System dynamics when in lock are determined by the amplifier/filter block. Its gain determines how much phase error exists between  $f_{in}$  and  $f_{out}$ , and filter characteristics shape the capture range and transient performance. This will be discussed in detail later.

**Loop Filter**

Fundamental loop characteristics such as capture range, loop bandwidth, capture time, and transient response are controlled primarily by the loop filter. The loop behavior is described by gains in each component block of Figure 8. The output to input ratio reflects a second order low pass filter in frequency response with a static gain of N:

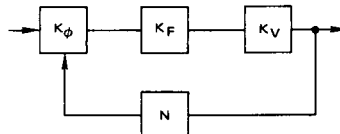
$$\frac{\theta_O(s)}{\theta_I(s)} = \frac{K_\phi K_F K_V}{s + \frac{K_\phi K_F K_V}{N}} \quad (1)$$

where:  $K_F = \frac{1 + T_1 s}{T_2 s}$  (2)

$T_1 = R_2 C$  and  $T_2 = R_1 C$  of Figure 4. Therefore,

$$\frac{\theta_O(s)}{\theta_I(s)} = \frac{N(1 + T_1 s)}{s^2 N T_2 + T_1 s + 1} \quad (3)$$

**FIGURE 8 — GAIN CONSTANTS**



$K_\phi$  = Phase Detector Gain (volts/radian)  
 $K_F$  = Amplifier/Filter Gain  
 $K_V$  = VCO Gain (radians/second/volt)  
 $N$  = Integer Divisor

Both  $\omega_n$  (loop bandwidth or natural frequency) and  $\zeta$  (damping factor) are particularly important in the transient response to a step input of phase or frequency (Figure 9), and are defined as:

$$\omega_n = \sqrt{\frac{K_\phi K_V}{N T_2}} \quad (4)$$

$$\zeta = \sqrt{\frac{K_\phi K_V}{N T_2} \left( \frac{T_1}{2} \right)} \quad (5)$$

Using these terms in Equation 3,

$$\frac{\theta_O(s)}{\theta_I(s)} = \frac{N(1 + T_1 s)}{\omega_n^2 s^2 + \frac{2\zeta s}{\omega_n} + 1} \quad (6)$$

In a well defined system controlling factors such as  $\omega_n$  and  $\zeta$  may be chosen either from a transient basis (time domain response) or steady state frequency plot (roll-off point and peaking versus frequency). Once these two design goals are defined, synthesis of the filter is relatively straight-forward.

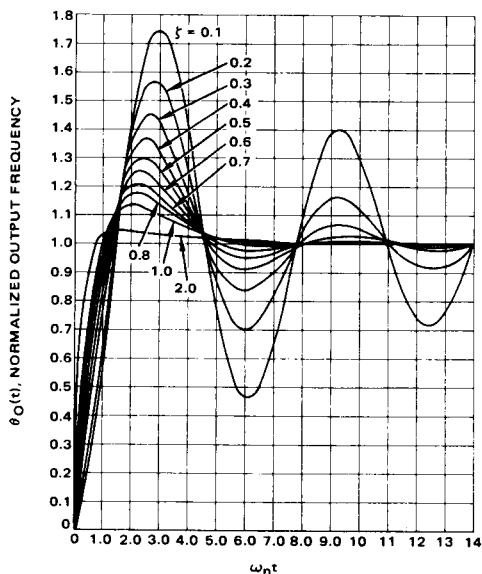
Constants  $K_\phi$ ,  $K_V$ , and  $N$  are usually fixed due to other design constraints, leaving  $T_1$  and  $T_2$  as variables to set  $\omega_n$  and  $\zeta$ . Since only  $T_2$  appears in Equation 4, it is the easiest to solve for initially.

$$T_2 = \frac{K_\phi K_V}{N \omega_n^2} \quad (7)$$

From Equation 5, we find

$$T_1 = \frac{2\zeta}{\omega_n} \quad (8)$$

FIGURE 9 — TYPE 2 SECOND ORDER STEP RESPONSE



Using relationships 7 and 8, actual resistor values may be computed:

$$R_1 = \frac{K\phi K_V}{N\omega_n^2 C} \quad (9)$$

$$R_2 = \frac{2\zeta}{\omega_n C} \quad (10)$$

Although fundamentally the range of  $R_1$  and  $R_2$  may be from several hundred to several thousand ohms, sideband considerations usually force the value of  $R_1$  to be set first, and then  $R_2$  and  $C$  computed.

$$C = \frac{K\phi K_V}{N\omega_n^2 R_1} \quad (11)$$

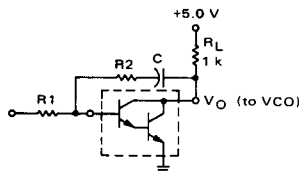
Calculation of passive components  $R_2$  and  $C$  (in synthesizers) is complicated by incomplete information on  $N$ , which is variable, and the limits of  $\omega_n$  and  $\zeta$  during that variance. Equally important are changes in  $K_V$  over the output frequency range. Minimum and maximum values of  $\omega_n$  and  $\zeta$  can be computed from Equations 4 and 5 when the appropriate worst case numbers are known for all the factors.

Amplifier/filter gain usually determines how much phase error exists between  $f_{in}$  and  $f_{out}$ , and the filter characteristic shapes capture range and transient performance. A relatively simple, low gain amplifier may usually be used in the loop since many designs are not constrained so much by phase error as by the need to make  $f_{in}$  equal  $f_{out}$ . Unnecessarily high gains can cause

problems in linear loops when the system is out of lock if the amplifier output swing is not adequately restricted since integrating operational amplifier circuits will latch up in time and effectively open the loop.

The internal amplifier included in the MC4344/4044 may be used effectively if its limits are observed. The circuit configuration shown in Figure 10 illustrates the placement of  $R_1$ ,  $R_2$ ,  $C$ , and load resistor  $R_L$  ( $1\text{ k}\Omega$ ). Due to the non-infinite gain of this stage ( $A_V \approx 30$ ) and other non-ideal characteristics, some restraint must be placed on passive component selection. Foremost is a lower limit on the value of  $R_2$  and an upper limit on  $R_1$ . Placed in order of priority, the recommendations are as follows: (a)  $R_2 > 50\ \Omega$ , (b)  $R_1/R_2 \leq 10$ , (c)  $1\text{ k}\Omega < R_1 < 5\text{ k}\Omega$ .

FIGURE 10 — USING MC4344/4044 LOOP AMPLIFIER



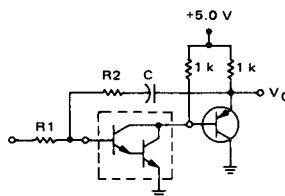
Limit (c) is the most flexible and may be violated with either higher sidebands and phase error ( $R_1 > 5\text{ k}\Omega$ ) or lower phase detector gain ( $R_1 < 1\text{ k}\Omega$ ). If limit (b) is exceeded, loop bandwidth will be less than computed and may not have any similarity to the prediction. For an accurate reproduction of calculated loop characteristics one should go to an operational amplifier which has sufficient gain to make limit (b) readily satisfied. Limit (a) is very important because  $T_1$  in Equation 5 is in reality composed of three elements:

$$T_1 = C \left( R_2 - \frac{1}{g_m} \right) \quad (12)$$

where  $g_m$  = transconductance of the common emitter amplifier.

Normally  $g_m$  is large and  $T_1$  nearly equals  $R_2 C$ , but resistance values below  $50\ \Omega$  can force the phase-compensating "zero" to infinity or worse (into the right half plane) and give an unstable system. The problem can be circumvented to a large degree by buffering the feedback with an emitter follower (Figure 11). Inequality (a) may then be reduced by at least an order of magnitude ( $R_2 > 5\ \Omega$ ) keeping in mind that electrolytic capacitors used

FIGURE 11 — AMPLIFIER CAPABLE OF HANDLING LOWER  $R_2$



as  $C$  may approach this value by themselves at the frequency of interest ( $\omega_n$ ).

Larger values of  $R_1$  may be accommodated by either using an operational amplifier with a low bias current ( $I_b < 1.0 \mu A$ ) as shown in Figure 12 or by buffering the internal Darlington pair with an FET (Figure 13). It is vitally important, however, that the added device be operated at zero  $V_{GS}$ . Source resistor  $R_4$  should be adjusted for this condition (which amounts to  $I_{DSS}$  current for the FET). This insures that the overall amplifier input threshold remains at the proper potential of approximately two base-emitter drops. Use of an additional emitter follower instead of the FET and  $R_4$  (Figure 14) gives a threshold near the upper limit of the phase detector charge pump, resulting in an extremely unsymmetrical phase detector gain in the pump up versus pump down mode. It is not unusual to note a 5:1 difference in  $K_\phi$  for circuits having the bipolar buffer stage. If the initial design can withstand this variation in loop gain and remain stable, the approach should be considered since there are no critical adjustments as in the FET circuit.

FIGURE 12 — USING AN OPERATIONAL AMPLIFIER TO EXTEND THE VALUE OF  $R_1$

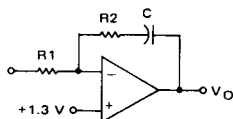


FIGURE 13 — FET BUFFERING TO RAISE AMPLIFIER INPUT IMPEDANCE

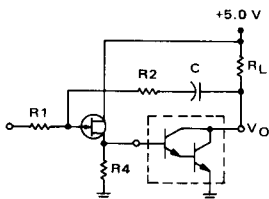
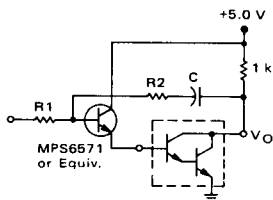


FIGURE 14 — EMITTER FOLLOWER BUFFERING OF AMPLIFIER INPUT



## DESIGN PROBLEMS AND THEIR SOLUTIONS

### Dynamic Range

A source of trouble for all phase-locked loops, as well as most electronics is simply overload or lack of sufficient dynamic range. One limit is the amplifier output drive to the VCO. Not only must a designer note the outside limits of the dc control voltage necessary to give the output frequency range, he must also account for the worst case of overshoot expected for the system. Relatively large damping factors ( $\zeta = 0.5$ ) can contribute significant amounts of overshoot (30%). To be prepared for the worst case output swing the amplifier should have as much margin to positive and negative limits as the expected swing itself. That is, if a two-volt swing is sufficient to give the desired output frequency excursion, there should be at least a two-volt cushion above and below maximum expected steady-state values on the control line.

This increase in range, in order to be effective, must of course be followed by an equivalent range in the VCO or there is little to be gained. Any loss in loop gain will in general cause a decrease in  $\zeta$  and a consequent increase in overshoot and ringing. If the loss in gain is caused by saturation or near saturation conditions, the problem tends to accelerate towards a situation where the system settles in not only a slow but oscillator manner as well.

Loss of amplifier gain may not be due entirely to normal system damping considerations. In loops employing digital phase detectors, an additional problem is likely to appear. This is due to amplifier saturation during a step input when there is a maximum phase detector output simultaneous with a large transient overshoot. The phase detector square wave rides on top of the normal transient and may even exceed the amplifier output limits imposed above. Since the input frequency will exceed the  $R_2C$  time constant, gain  $K_F$  for these annoying pulses will be  $R_2/R_1$ . Ordinarily this ratio will be less than 1, but some circumstances dictate a low loop gain commensurate with a fairly high  $\omega_n$ . For these cases,  $R_2/R_1$  may be higher than 10 and cause pulse-wise saturation of the amplifier. Since the dc control voltage is an average of phase detector pulses, clipping can be translated into a reduction in gain with all the "benefits" already outlined, i.e., poor settling time. An easy remedy to apply in many cases is a simple RC low pass section preceding or together with the integrator-lag section. To make transient suppression independent of amplifier response, the network may be imbedded within the input resistor  $R_1$  (Figure 15) or be implemented by placing a feedback capacitor across  $R_2$  (Figure 16). Besides rounding off and inhibiting pulses, these networks add an additional pole to the loop and may cause further overshoot if the cutoff frequency ( $\omega_c$ ) is too close to  $\omega_n$ . If at all possible the cutoff point should be five to ten times  $\omega_n$ . How far  $\omega_c$  can be placed from  $\omega_n$  depends on the input frequency relationship to  $\omega_n$  since  $f_{in}$  is, after all, what is being filtered. A side benefit of this simple RC pulse "flattener" is a reduction in  $f_{in}$  sidebands around  $f_{out}$  for synthe-



sizers with  $N > 1$ . However, a series of RC filters is not recommended for either extended pulse suppression or sideband improvement as excess phase will begin to build up at the loop crossover ( $\approx \omega_n$ ) and tend to cause instability. This will be discussed in more detail later.

FIGURE 15 — IMPROVED TRANSIENT SUPPRESSION WITH  $R1 - C_c$

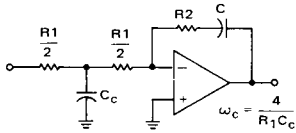
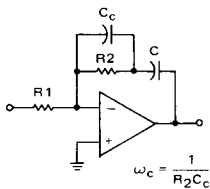


FIGURE 16 — IMPROVED TRANSIENT SUPPRESSION WITH  $R2 - C_c$



**Spurious Outputs**

Although the major problem in phase-locked loop design is defining loop gain and phase margin under dynamic operating conditions, high-quality synthesizer designs also require special consideration to minimize spurious spectral components — the worst of which is reference-frequency sidebands. Requirements for good sideband suppression often conflict with other performance goals — loop dynamic behavior, suppression of VCO noise, or suppression of other in-loop noise. As a result, most synthesizer designs require compromised specifications. For a given set of components and loop dynamic conditions, reference sidebands should be predicted and checked against design specifications before any hardware is built.

Any steady-state signal on the VCO control will produce sidebands in accordance with normal FM theory. For small spurious deviations on the VCO, relative sideband-to-carrier levels can be predicted by:

$$\frac{\text{sidebands}}{\text{carrier}} \cong \frac{V_{\text{ref}} K_V}{2\omega_{\text{ref}}} \tag{13}$$

where  $V_{\text{ref}}$  = peak voltage value of spurious frequency at the VCO input.

Unwanted control line modulation can come from a variety of sources, but the most likely cause is phase detector pulse components feeding through the loop fil-

ter. Although the filter does establish loop dynamic conditions, it leaves something to be desired as a low pass section for reference frequency components.

For the usual case where  $\omega_{\text{ref}}$  is higher than  $1/T_2$ , the  $K_F$  function amounts to a simple resistor ratio:

$$K_F(j\omega) \Big|_{\omega = \omega_{\text{ref}}} \cong - \frac{R_2}{R_1} \tag{14}$$

By substitution of Equations 9 and 10, this signal transfer can be related to loop parameters.

$$K_F(j\omega) \Big|_{\omega = \omega_{\text{ref}}} \cong \frac{2\zeta N\omega_n}{K_\phi K_V} = \frac{V_{\text{ref}}}{V_\phi} \tag{15}$$

where  $V_{\text{ref}}$  = peak value of reference voltage at the VCO input, and  
 $V_\phi$  = peak value of reference frequency voltage at the phase detector output.

Sideband levels relative to reference voltage at the phase detector output can be computed by combining Equations 13 and 15:

$$\frac{\text{sideband level}}{f_{\text{out level}}} = V_\phi \left( \frac{\zeta N\omega_n}{\omega_{\text{ref}} K_\phi} \right) \tag{16}$$

From Equation 16 we find that for a given phase detector, a given value of  $R_1$  (which determines  $V_\phi$ ), and given basic system constraints ( $N, f_{\text{ref}}$ ), only  $\zeta$  and  $\omega_n$  remain as variables to diminish the sidebands. If there are few limits on  $\omega_n$ , it may be lowered indefinitely until the desired degree of suppression is obtained. If  $\omega_n$  is not arbitrary and the sidebands are still objectionable, additional filtering is indicated.

One item worthy of note is the absence of  $K_V$  in Equation 16. From Equation 15 it might be concluded that decreasing  $K_V$  would be another means for reducing spurious sidebands, but for constant values of  $\zeta$  and  $\omega_n$  this is not a free variable. In a given loop, varying  $K_V$  will certainly affect sideband voltage, but will also vary  $\zeta$  and  $\omega_n$ .

On the other hand, the choice of  $\omega_n$  may well affect spectral purity near the carrier, although reference sideband levels may be quite acceptable.

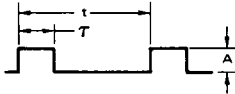
In computing sideband levels, the value of  $V_\phi$  must be determined in relation to other loop components. Residual reference frequency components at the phase detector output are related to the dc error voltage necessary to supply charge pump leakage current and amplifier bias current. From these average voltage figures, spectral components of the reference frequency and its harmonics can be computed using an approximation that the phase detector output consists of square waves  $\tau$  seconds

wide repeated at  $t$  second intervals (Figure 17). A Fourier analysis can be summarized for small ratios of  $\tau/t$  by:

- (1) the average voltage ( $V_{avg}$ ) is  $A(\tau/t)$
- (2) the peak reference voltage value ( $V_\phi$ ) is twice  $V_{avg}$ , and
- (3) the second harmonic ( $2f_{ref}$ ) is roughly equal in amplitude to the fundamental.

By knowing the requirements for (1) due to amplifier bias and leakage currents, values for (2) and (3) are uniquely determined.

FIGURE 17 — PHASE DETECTOR OUTPUT



An example of this sideband approximation technique can be illustrated using the parameters specified for the synthesizer design included in the applications information section.

$$\begin{aligned}
 N_{max} &= 30 & \omega_n &= 4500 \text{ rad/s} \\
 K_V &= 11.2 \times 10^6 \text{ rad/s/V} & R_1 &= 2 \text{ k}\Omega \\
 K_\phi &= 0.12 \text{ V/rad} & f_{ref} &= 100 \text{ kHz} \\
 \zeta &= 0.8
 \end{aligned}$$

Substituting these numbers into Equation 16:

$$\begin{aligned}
 \frac{\text{sideband}}{f_{out}} &= V_\phi \frac{(0.8)(30)(4500)}{2\pi(10^5)(0.111)} & (17) \\
 &= V_\phi (1.55) & (18)
 \end{aligned}$$

The result illustrates how much reference feedthrough will affect sideband levels. If 1.0 mV peak of reference appears at the output of the phase detector, the nearest sideband will be down 56.2 dB.

If the amplifier section included in the MC4344/4044 is used, with  $R_L = 1 \text{ k}\Omega$ , some approximations of the value of  $V_\phi$  can be made based on the input bias current and the value of  $R_1$ . The phase detector must provide sufficient average voltage to supply the amplifier bias current,  $I_b$ , through  $R_1$ ; when the bias current is about 5.0  $\mu\text{A}$  and  $R_1$  is 2  $\text{k}\Omega$ ,  $V_{avg}$  must be 10 mV. From the assumptions earlier concerning the Fourier transform, and with the help of Figure 18, we can see that the phase detector duty cycle will be about 1.7% ( $A = 0.6 \text{ V}$ ), giving a fundamental (reference) of 20 mV peak. If this value for  $V_\phi$  is substituted into Equation 18, the resulting sideband ratio represents 30 dB suppression due to this component alone.

In addition to the amplifier bias current, another factor to consider is transistor Q5 reverse leakage current  $I_L$  flowing into pin 10 of the MC4344/4044 charge pump.  $I_L$  is generally less than 1.0  $\mu\text{A}$  and is no more than 5.0  $\mu\text{A}$  over the temperature range. A typical design value for 25°C is 0.1  $\mu\text{A}$ . Both  $I_L$  and amplifier bias current  $I_b$  are

in a direction to deplete the charge on filter capacitor C. A second charge pump leakage,  $I_L'$ , attributed by diode CR1 flows out of pin 5. This current, however, is in a direction to help supply  $I_b$  and  $I_L$  and thus tends to minimize the discharge of C. Typically  $I_L'$  is much less than  $I_L$  and, since it is also in a direction to minimize discharge of the filter capacitor, it will be ignored in the following discussion. The total charge removed from C must be replaced by current supplied by the charge pump during the next up-date opportunity. This current flows through  $R_1$ . To minimize the effects of  $I_b$  and  $I_L$  a relative small value of  $R_1$  should be chosen. A minimum value of 1  $\text{k}\Omega$  is a good choice.

FIGURE 18 — OUTPUT ERROR CHARACTERISTICS

| DUTY CYCLE (%) | PHASE ERROR (Deg) | $V_{avg}$ (mV) | $V_\phi(\text{peak})$ (mV) |
|----------------|-------------------|----------------|----------------------------|
| 0.1            | 0.36              | 0.6            | 1.2                        |
| 0.2            | 0.72              | 1.2            | 2.4                        |
| 0.3            | 1.08              | 1.8            | 3.6                        |
| 0.4            | 1.44              | 2.4            | 4.8                        |
| 0.5            | 1.80              | 3.0            | 6.0                        |
| 0.6            | 2.16              | 3.6            | 7.2                        |
| 0.7            | 2.52              | 4.2            | 8.4                        |
| 0.8            | 2.88              | 4.8            | 9.6                        |
| 0.9            | 3.24              | 5.4            | 10.8                       |
| 1.0            | 3.60              | 6.0            | 12.0                       |
| 2.0            | 7.2               | 12.0           | 24.0                       |
| 3.0            | 10.8              | 18.0           | 35.9                       |
| 4.0            | 14.4              | 24.0           | 47.9                       |
| 5.0            | 18.0              | 30.0           | 59.8                       |
| 6.0            | 21.6              | 36.0           | 71.6                       |
| 7.0            | 25.2              | 42.0           | 83.3                       |
| 8.0            | 28.8              | 48.0           | 95.0                       |
| 9.0            | 32.4              | 54.0           | 106.6                      |
| 10.0           | 36.0              | 60.0           | 118.0                      |

After values for C and  $R_2$  have been computed on the basis of loop dynamic properties, the overall sideband to  $f_{out}$  ratio computation can be simplified.

Since

$$\begin{aligned}
 V_\phi &= 2 V_{avg} & &= 2R_1 (I_b + I_L) \left(\frac{R_2}{R_1}\right) \\
 V_{avg} &= (I_b + I_L) R_1 \\
 V_\phi &= 2 (I_b + I_L) R_1 & &= 2R_2 (I_b + I_L) \\
 V_{ref} &= V_\phi \left(\frac{R_2}{R_1}\right)
 \end{aligned}$$

we find that

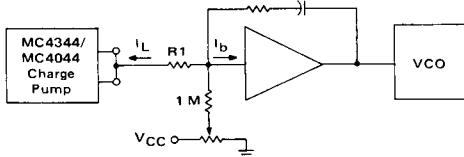
$$\frac{\text{sideband}}{f_{out}} = \frac{V_{ref}K_V}{2\omega_{ref}} \quad (19)$$

$$\frac{\text{sideband}}{f_{out}} = \frac{2R_2(I_b + I_L)K_V}{2\omega_{ref}} \quad (20)$$

Equation 20 indicates that excellent suppression could be achieved if the bias and leakage terms were nulled by current summing at the amplifier input (Figure 19). This has indeed proved to be the case. Experimental results indicate that greater than 60 dB rejection can routinely

be achieved at a constant temperature. However when nulling fairly large values ( $> 100 \text{ nA}$ ), the rejection becomes quite sensitive since leakages are inherently a function of temperature. This technique has proved useful in achieving improved system performance when used in conjunction with good circuit practice and reference filtering.

FIGURE 19 — COMPENSATING FOR BIAS AND LEAKAGE CURRENT



**Additional Loop Filtering**

So far, only the effects of fundamental loop dynamics on resultant sidebands have been considered. If further sideband suppression is required, additional loop filtering is indicated. However, care must be taken in placement of any low pass rolloff with regard to the loop natural frequency ( $\omega_n$ ). On one hand, the "corner" should be well below (lower than)  $\omega_{ref}$  and yet far removed (above) from  $\omega_n$ . Although no easy method for placing the roll-off point exists, a rule of thumb that usually works is:

$$\omega_c = 5\omega_n \quad (21)$$

Reference frequency suppression per pole is the ratio of  $\omega_c$  to  $\omega_{ref}$ .

$$S_{dB} \approx n \cdot 20 \log_{10} \left( \frac{\omega_c}{\omega_{ref}} \right) \quad (22)$$

where  $n$  is the number of poles in the filter.

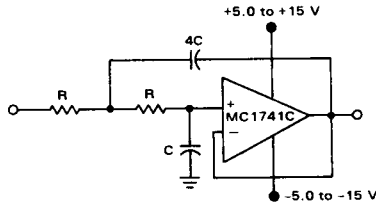
Equation 22 gives the additional loop suppression to  $\omega_{ref}$ ; this number should be added to whatever suppression already exists.

For non-critical applications, simple RC networks may suffice, but if more than one section is required, loop dynamics undergo undesirable changes. Loop damping factor decreases, resulting in a high percentage of overshoot and increased ringing since passive RC sections tend to accumulate phase shift more rapidly than signal suppression and part of this excess phase subtracts from the loop phase margin. Less phase margin translates into a lower damping factor and can, in the limit, cause outright oscillation.

A suitable alternative is an active RC section, Figure 20, compatible with the existing levels and voltages. An active two pole filter (second order section) can realize a more gradual phase shift at frequencies less than the cutoff point and still get nearly equal suppression at frequencies above the cutoff point. Sections designed with a slight amount of peaking ( $\zeta \approx 0.5$ ) show a good compromise between excess phase below cutoff ( $\omega_c$ ), without peaking enough to cause any danger of raising the loop gain for frequencies above  $\omega_n$ . A fairly non-critical section may simply use an emitter follower as the active device

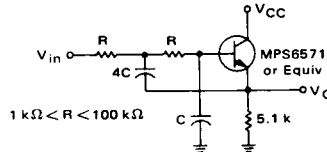
with two resistors and capacitors completing the circuit (Figure 21). This provides a  $-12 \text{ dB/octave}$  ( $-40 \text{ dB/decade}$ ) rolloff characteristic above  $\omega_n$ , though the attenuation may be more accurately determined by Equation 22. If the sideband problem persists, an additional section may be added in series with the first. No more than two sections are recommended since at that time either (1) the constraint between  $\omega_n$  and  $\omega_{ref}$  is too close, or (2) reference voltage is modulating the VCO from a source other than the phase detector through the loop amplifier.

FIGURE 20 — OPERATIONAL AMPLIFIER LOW PASS FILTER



1. Choose R  
 $1 \text{ k}\Omega < R < 1 \text{ M}\Omega$
2.  $C = \frac{0.5}{\omega_c R}$

FIGURE 21 — EMITTER FOLLOWER LOW PASS FILTER



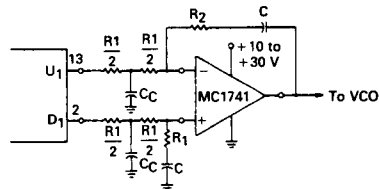
NOTE: If  $V_D \approx V_{CC} - 1.0 \text{ V}$ , this stage is susceptible to power supply noise.

Operation without charge pump phase detector #1 of the MC4344/4044 can be implemented quite successfully in many applications without using the charge pump and internal darlington amplifier approach. An operational amplifier filter can be used to process the error information appearing at U1 and D1 (pins 13 and 2) directly (Figure 22). This phase detector/filter approach offers a potentially superior performing system because:

- a. Charge pump delay time is eliminated.
- b. Charge pump input signed threshold level need not be overcome before error information is obtained.

This can result in a substantial improvement in the

FIGURE 22 — TYPICAL FILTER AND SUMMING NETWORK



4044's transfer function linearity in the vicinity of zero phase error between the R and V inputs.

- c. The filter amplifier ground location can be separated from the phase detector ground.
- d. An "optimum" filter amplifier input threshold of approximately two diode drops need not be established.

The filter discussions and relationships developed for integrator-log filter sections can be applied to the system of Figure 22 and the previously derived equations can be used to determine values for R1, R2 and C.

It may be desirable to split each of the R1 resistors and incorporate a capacitor to ground in a manner similar to that shown in Figure 15. This should improve transient suppression and provide integration of the U1 and D1 signals to better enable the operational amplifier to develop corrective error information from very narrow U1 and D1 pulse widths.

Phase error for the circuit in Figure 22 will result from input offset voltage in the operational amplifier, resistor mismatch and mismatch between the phase detector output states appearing at U1 and D1. Phase error can be trimmed to zero initially by adjusting either the amplifier input offset or one of the R1 resistors.

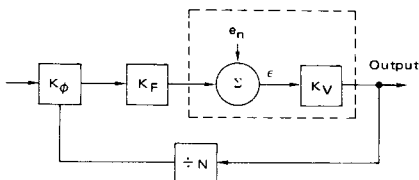
**VCO Noise**

Effects of noise within the VCO itself can be evaluated by considering a closed loop situation with an external noise source,  $e_n$ , introduced at the VCO (Figure 23). Resultant modulation of the VCO by error voltage,  $\epsilon$ , is a second order high pass function:

$$\frac{\epsilon}{e_n} = \frac{S^2}{S^2 + \frac{ST_1K\phi KV}{T_2N} + \frac{K\phi KV}{T_2N}} \quad (23)$$

$$= \frac{S^2}{S^2 + 2\zeta\omega_n S + \omega_n^2}$$

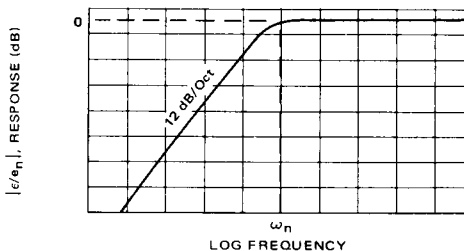
FIGURE 23 — EFFECTS OF VCO NOISE



$$\frac{\epsilon}{e_n} = \frac{S^2}{S^2 + 2\zeta\omega_n S + \omega_n^2}$$

This function has a slope of 12 dB/octave at frequencies less than  $\omega_n$  (loop natural frequency), as shown in Figure 24. This means that noise components in the VCO above  $\omega_n$  will pass unattenuated and those below will have some degree of suppression. Therefore choice of loop natural frequency may well rest on VCO noise quality.

FIGURE 24 — LOOP RESPONSE TO VCO NOISE

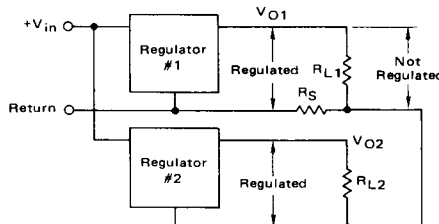


**Other Spurious Responses**

Spurious components appearing in the output spectrum are seldom due to reference frequency feedthrough alone. Modulation of any kind appearing on the VCO control line will cause spurious sidebands and can come in through the loop amplifier supply, bias circuitry in the control path, a translator, or even the VCO supply itself. Some VCOs have a relatively high sensitivity to power supply variation. This should be investigated and its effects considered. Problems of this nature can be minimized by operating all devices except the phase detector, charge pump, and VCO from a separate and well isolated supply. A common method uses a master supply of about 10 or 12 volts and two regulators to produce voltages for the PLL — one for all the logic (including the phase detector) and the other for all circuitry associated with the VCO control line.

Sideband and noise performance is also a function of good power supply and regulator layout. As mentioned earlier, extreme care should be exercised in isolating the control line voltage to the VCO from influences other than the phase detector. This not only means good voltage regulation but ac bypassing and adherence to good grounding techniques as well. Figure 25 shows two separate regulators and their respective loads. Resistor  $R_S$  is a small stray resistance due to a common thin ground return for both  $R_{L1}$  and  $R_{L2}$ . Any noise in  $R_{L2}$  is now reproduced (in a suppressed form) across  $R_{L1}$ . Load current from  $R_{L1}$  does not affect the voltage across  $R_{L2}$ . Even though the regulators may be quite good, they can hold  $V_O$  constant only across their outputs, not necessarily across the load (unless remote sensing is used).

FIGURE 25 — LOOP VOLTAGE REGULATION



One solution to the ground-coupled noise problem is to lay out the return path with the most sensitive regulated circuit at the farthest point from power supply entry as shown in Figure 26.

Even for regulated subcircuits, accumulated noise on the ground bus can pose major problems since although the cross currents do not produce a differential load voltage directly, they do produce essentially common mode noise on the regulators. Output differential load noise then is a function of the input regulation specification. By far the best way to sidestep the problem is to connect each subcircuit ground to the power supply entry return line as shown in Figure 27.

FIGURE 26 — REGULATOR LAYOUT

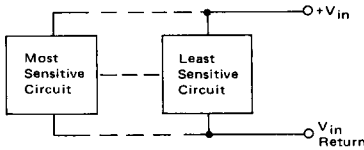
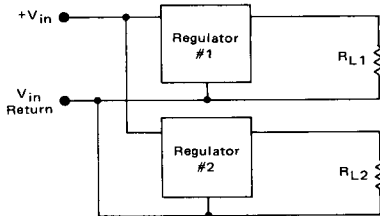
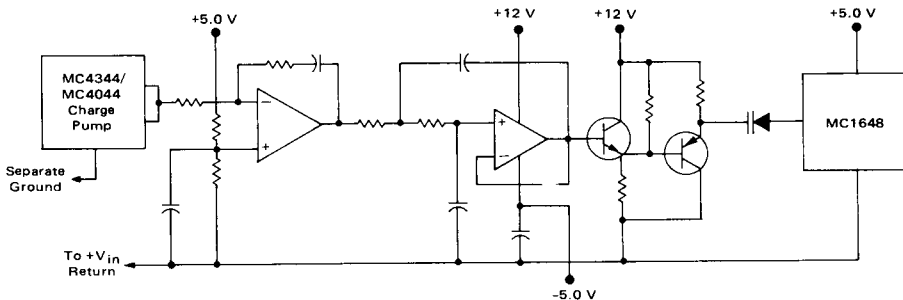


FIGURE 27 — REGULATOR GROUND CONNECTION



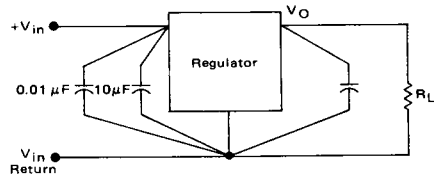
In Figures 25 and 27,  $R_{L1}$  and  $R_{L2}$  represent component groups in the system. The designer must insure that all ground return leads in a specific component group are returned to the common ground. Probably the most overlooked components are bypass capacitors. To minimize sidebands, extreme caution must be taken in the area immediately following the phase detector and through the VCO. A partial schematic of a typical loop amplifier and filter is shown in Figure 28 to illustrate the common grounding technique.

FIGURE 28 — PARTIAL SCHEMATIC OF LOOP AMPLIFIER AND FILTER



Bypassing in a phase-locked loop must be effective at both high frequencies and low frequencies. One capacitor in the 1.0-to-10  $\mu\text{F}$  range and another between 0.01 and 0.001  $\mu\text{F}$  are usually adequate. These can be effectively utilized both at the immediate circuitry (between supply and common ground) and the regulator if it is some distance away. When used at the regulator, a single electrolytic capacitor on the output and a capacitor pair at the input is most effective (Figure 29). It is important, again, to note that these bypasses go from the input/output pins to as near the regulator ground pin as possible.

FIGURE 29 — SUGGESTED BYPASSING PROCEDURE

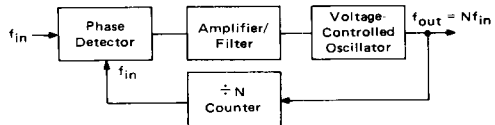


APPLICATIONS INFORMATION

Frequency Synthesizers

The basic PLL discussed earlier is actually a special case of frequency synthesis. In that instance,  $f_{out} = f_{in}$ , although normally a programmable counter in the feedback loop insures the general rule that  $f_{out} = Nf_{in}$  (Figure 30). In the synthesizer  $f_{in}$  is usually constant (crystal controlled) and  $f_{out}$  is changed by varying the programmable divider ( $\div N$ ). By stepping  $N$  in integer increments, the output frequency is changed by  $f_{in}$  per increment. In com-

FIGURE 30 — PHASE-LOCKED LOOP WITH PROGRAMMABLE COUNTER



munication use, this input frequency is called the "channel spacing" or, in general, it is the reference frequency.

There is essentially no difference in loop dynamic problems between the basic PLL and synthesizers except that synthesizer designers must contend with problems peculiar to loops where N is variable and greater than 1. Also, sidebands or spectral purity usually require special attention. These and other aspects are discussed in greater detail in AN-535. The steps for a suitable synthesis procedure may be summarized as follows:

**Synthesis Procedure**

1. Choose input frequency. ( $f_{ref}$  = channel spacing)
2. Compute the range of digital division:

$$N_{max} = \frac{f_{max}}{f_{ref}}$$

$$N_{min} = \frac{f_{min}}{f_{ref}}$$

3. Compute needed VCO range:

$$(2f_{max} - f_{min}) < f_{VCO} < (2f_{min} - f_{max})$$

4. Choose minimum  $\zeta$  from transient response plot, Figure 9. A good starting point is  $\zeta = 0.5$ .
5. Choose  $\omega_n$  from needed response time (Figure 9):

$$\omega_n = \frac{\omega_n t}{t}$$

6. Compute C:

$$C = \frac{K_\phi K_V}{N_{max} \omega_n^2 R_1}$$

7. Compute  $R_2$ :

$$R_2 = \frac{2\zeta_{min}}{\omega_n C}$$

8. Compute  $\zeta_{max}$ :

$$\zeta_{max} = \zeta_{min} \sqrt{\frac{N_{max}}{N_{min}}}$$

9. Check transient response of  $\zeta_{max}$  for compatibility with transient specification.
10. Compute expected sidebands:

$$\frac{\text{sideband}}{f_{out}} \cong \frac{(I_b + I_L)R_2 K_V}{\omega_{ref}} \quad (A)$$

( $I_L$  is about 100 nA at  $T_J = 25^\circ\text{C}$ .)

11. If step 10 yields larger sidebands than are acceptable, add a single pole at the loop amplifier by splitting  $R_1$  and adding  $C_c$  as shown in Figure 15:

$$C_c \cong \frac{0.8}{R_1 \omega_n}$$

Added sideband suppression (dB) is:

$$\text{dB} \cong 20 \log_{10} \frac{1}{\sqrt{1 + \frac{\omega_{ref}^2}{25(\omega_n)^2}}} \quad (B)$$

12. If step 11 still does not give the desired results, add a second order section at  $\omega_c = 5 \omega_n$  using either the configuration of Figure 20 or 21. The expected improvement is twice that of the single pole in step 11.

$$\text{dB} \cong 40 \log_{10} \frac{1}{\sqrt{1 + \frac{\omega_{ref}^2}{25(\omega_n)^2}}} \quad (C)$$

Total sideband rejection is then the total of  $20 \log_{10}(A) + (B) + (C)$ .

**Design Example (Figure 31)**

Assume the following requirements:

Output frequency,  $f_{out} = 2.0 \text{ MHz}$  to  $3.0 \text{ MHz}$

Frequency steps,  $f_{in} = 100 \text{ kHz}$

Lockup time between channels (to 5%) = 1.0 ms

Overshoot < 20%.

Minimum sideband suppression = -30 dB

From the steps of the synthesis procedure:

1.  $f_{ref} = f_{in} = 100 \text{ kHz}$

$$2. N_{max} = \frac{f_{max}}{f_{ref}} = \frac{3.0 \text{ MHz}}{0.1 \text{ MHz}} = 30$$

$$N_{min} = \frac{f_{min}}{f_{ref}} = \frac{2.0 \text{ MHz}}{0.1 \text{ MHz}} = 20$$

3. VCO range:

The VCO output frequency range should extend beyond the specified minimum-maximum limits to accommodate the overshoot specification. In this instance  $f_{out}$  should be able to cover an additional 20% on either end. End limits on the VCO are:

$$f_{outmax} \cong 3.0 + 0.2(1.0) = 3.2 \text{ MHz}$$

$$f_{outmin} \cong 2.0 - 0.2(1.0) = 1.8 \text{ MHz}$$

This VCO range ( $\approx 1.8:1$ ) is realizable with the MC4324/4024 voltage controlled multivibrator. From Figure 5 of the MC4324/4024 data sheet we find the required tuning capacitor value to be 120 pF and the VCO gain,  $K_V$ , typically  $11 \times 10^6 \text{ rad/s/v}$ .

4. From the step response curve of Figure 9,  $\zeta = 0.8$  will produce a peak overshoot less than 20%.
5. Referring to Figure 9, overshoot with  $\zeta = 0.8$  will settle to within 5% at  $\omega_n t = 4.5$ . Since the required lock-up time is 1.0 ms,

$$\omega_n = \frac{\omega_n t}{t} = \frac{4.5}{0.001} = (4.5)(10^3) \text{ rad/s}$$

6. In order to compute C, phase detector gain and R<sub>1</sub> must be selected. Phase detector gain, K<sub>φ</sub>, for the MC4344/4044 is approximately 0.1 volt/radian with R<sub>1</sub> = 1 kΩ. Therefore,

$$C = \frac{(0.1)(11 \times 10^6)}{(30)(4.5 \times 10^3)^2(10^3)} = 1.8 \mu\text{F}$$

7. At this point, R<sub>2</sub> can be computed:

$$R_2 = \frac{2\zeta_{\min}}{\omega_n C} = \frac{1.6}{(4.5 \times 10^3)(1.8 \times 10^{-6})} = 200 \Omega$$

$$8. \zeta_{\max} = \zeta_{\min} \sqrt{\frac{N_{\max}}{N_{\min}}} = 0.98$$

9. Figure 9 shows that ζ = 0.98 will meet the settling time requirement.

10. Sidebands may be computed for two cases: (1) with I<sub>L</sub> (charge pump leakage current) nominal (100 nA), and (2) with I<sub>L</sub> maximum (5.0 μA). A value of 5 μA will also be assumed for the amplifier bias current, i<sub>b</sub>.

$$\left. \frac{\text{sideband}}{f_{\text{out}}} \right|_{\max} = \frac{(10 \times 10^{-6})(200)(11 \times 10^6)}{6.28 \times 10^5} \cong 35 \times 10^{-3}$$

The sideband-to-center frequency ratio nominally will be:

$$\left. \frac{\text{sideband}}{f_{\text{out}}} \right|_{\text{nom}} = \frac{5.1}{10} \times 35 \times 10^{-3}$$

$$= 20 \log_{10}(17.85 \times 10^{-3}) \cong -35 \text{ dB}$$

If desired additional sideband filtering can be obtained as noted in steps 11 and 12.

11. By splitting R<sub>1</sub> and C<sub>c</sub>, further attenuation can be gained. The magnitude of C<sub>c</sub> is approximately:

$$C_c = \frac{0.8}{R_1 \omega_n} = \frac{0.8}{(10^3)(4.5)(10^3)} \cong 0.18 \mu\text{F}$$

Improvement in sidebands will be:

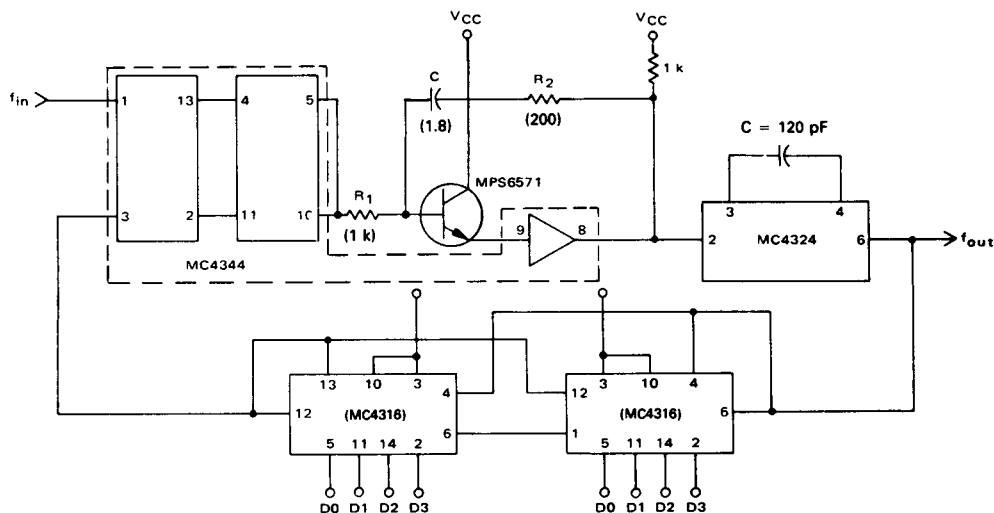
$$20 \log_{10} \frac{1}{\sqrt{1 + \frac{(2\pi \times 10^5)^2}{25(4.5 \times 10^3)^2}}} = -28 \text{ dB}$$

Nominal suppression is now -63 dB. Worst-case is 6 dB higher than nominal suppression of -57 dB. This is well within the -30 dB design requirement, step 12 is included for completeness only.

12. Attenuation of a second order filter is double that of the single order filter section described in step 11. The calculations for a second order filter indicate an additional -56 dB of sideband rejection. Figures 20 and 21 show two second order filter configurations. If R is assigned a value of 10 kΩ then C may be calculated.

$$C = \frac{0.1}{\omega_n R} = \frac{0.1}{(4.5 \times 10^3)(10^4)} = 0.0022 \mu\text{F}$$

FIGURE 31 — CIRCUIT DIAGRAM OF TYPE 2 PHASE-LOCKED LOOP







its complement,  $\overline{DGATE}$ , serve to initialize the circuitry and insure that the first transition of the data block (a phase transition) is ignored. The MC7493 binary counter and the G5-G12 latch generate a suitable signal for gating out G3 pulses caused by phase transitions at the end of a data cell, such as the one shown dashed in row 6.

The initial data pulse from G3 sets G12 low and is combined with DGATE in G7 to reset the counter to its zero state. Subsequent VCM clock pulses now cycle the counter and approximately one-third of the way through the next data cell the counter's full state is decoded by G11, generating a negative transition. This causes G12 to go high, removing the inhibit signal until it is again reset by the next data transition. This pulse also resets the counter, continuing the cycle and generating a positive pulse at the midpoint of each data cell as required.

Acquisition time is reduced if the loop is locked to a frequency approximately the same as the expected data rate during inter-block gaps. In Figure 32, this is achieved by operating the remaining half of the dual VCM at slightly less than the data rate and applying it to the reference input of the phase detector via the G8-G9-G10 data selector. When data appears, DGATE and  $\overline{DGATE}$  cause the output of G3 to be selected as the reference input to the loop.

The loop parameters are selected as a compromise between fast acquisition and jitter-free tracking once synchronization is achieved. The resulting filter component values indicated in Figure 32 are suitable for recovering the clock from data recorded at a 120 kHz rate, such as would result in a tape system operating at 75 i.p.s. with a recording density of 1600 b.p.i. Synchronization is achieved by approximately the twenty-fourth bit time of the preamble. The relationship between system requirements and the design procedure is illustrated by the following sample calculation:

Assume a -3.0 dB loop bandwidth much less than the input data rate (= 120 kHz), say 10 kHz. Further, assume a damping factor of  $\zeta = 0.707$ . From the expression for loop bandwidth as a function of damping factor and undamped natural frequency,  $\omega_n$ , calculate  $\omega_n$  as:

$$\omega_{-3 \text{ dB}} = \omega_n \left( 1 + 2\zeta^2 + \sqrt{2 + 4\zeta^2 + 4\zeta^4} \right)^{1/2} \quad (24)$$

or for  $\omega_{-3 \text{ dB}} = (2\pi)10^4$  rad/s and  $\zeta = 0.707$ :

$$\omega_n = \frac{(2\pi)10^4}{2.06} = (3.05)10^4 \text{ rad/s}$$

As a rough check on acquisition time, assume that lockup should occur not later than half-way through a 40-bit preamble, or for twenty 8.34  $\mu$ s data periods.

$$\omega_n t = (3.05)10^4(20)(8.34)10^{-6} = 5.1 \quad (26)$$

From Figure 9, the output will be within 2 to 3% of its final value for  $\omega_n t \approx 5$  and  $\zeta = 0.707$ . The filter components are calculated by:

$$\frac{K_\phi K_V}{R_1 C_N} = \omega_n^2 \quad (27)$$

and

$$\frac{K_\phi K_V R_2}{R_1 N} = 2\zeta\omega_n \quad (28)$$

where

$$\begin{aligned} K_\phi &= 0.115 \text{ v/rad} \\ K_V &= (18.2) 10^6 \text{ rad/s/volt} \\ N &= 24 = \text{Feedback divider ratio} \\ \omega_n &= (3.05) 10^4 \text{ rad/s} \\ \zeta &= 0.707 \\ \frac{K_\phi K_V}{N} &= \frac{(0.115)(18.2)10^6}{24} = (8.72)10^4 \end{aligned}$$

From Equation 27:

$$R_1 C = \frac{K_\phi K_V}{N \omega_n^2} = \frac{(8.72)10^4}{(3.05)^2 10^8} = (9.34)10^{-5}$$

From Equation 28:

$$\frac{R_2}{R_1} = \frac{2\zeta\omega_n N}{K_\phi K_V} = \frac{2(0.707)(3.05)10^4}{(8.72)10^4} = 0.494 \approx 1/2$$

Let  $R_1 = 3.0 \text{ k}\Omega$ ; then  $R_2 = 1.5 \text{ k}\Omega$  and

$$C = \frac{(9.34)10^{-5}}{(3.0)10^3} = (3.1)10^{-8}$$

or using a close standard value, use  $C = 0.033 \mu\text{F}$ . Now add the additional prefiltering by splitting  $R_1$  and selecting a time constant for the additional section so that it is large with respect to  $R_2 C_2$ .

$$10(1/2 R_1) C_C = R_2 C$$

or

$$C_C = \frac{2R_2 C}{10R_1} = \frac{2(1.5)10^3(3.3)10^{-8}}{10(3.0)10^3} = 3300 \text{ pF}$$

FIGURE 33 — TIMING DIAGRAM — CLOCK RECOVERY FROM PHASE-ENCODED DATA

